

# APPLICATIONS OF ARTIFICIAL POTENTIAL FUNCTION METHODS TO AUTONOMOUS SPACE FLIGHT

S.K. Scarritt\* and B.G. Marchand†

The goal of this investigation is to identify a systematic approach for the determination of accurate startup arcs for autonomous spacecraft path planning and guidance. This capability is of particular interest for on-demand onboard determination. Artificial potential function methods are common in the field of path planning. However, the resulting control requirements are not always feasible in practice due to various hardware and mission constraints. Still, the general concept is useful in the determination of suitable startup arcs for autonomous algorithms that are capable of addressing these actuator constraints on demand.

## INTRODUCTION

The success of iterative gradient based targeting algorithms, whether optimal or suboptimal, depends on the quality of the startup solution available. Thus, autonomous targeting<sup>1</sup> suggests autonomy in both the computational process used to identify a feasible or optimal solution, given some initial guess, and in the process of identifying the startup arc itself. Regardless of the targeting algorithm selected, the startup arc need not be completely feasible. However, the quality of the startup solution does influence the performance of gradient based targeting algorithms. Furthermore, the solution space explored by gradient based targeting methods is restricted to the immediate vicinity of the startup arc. This may ultimately limit the types of arcs identified by the targeting process.

Preliminary trajectory design is often accomplished through patched-conic approximations.<sup>2</sup> Of course, two-body patched-conic solutions propagated in a more complete  $n$ -body model, for  $n \geq 3$ , do not lead to feasible trajectory arcs since a discontinuity at the patch-point is generally expected. Iterative targeting algorithms, optimal or suboptimal, are necessary to re-acquire a feasible continuous solution in the full dynamical model. Ultimately, the accuracy of the patched-conic approximation varies according to the regime and any related mission requirements. Low-energy spacecraft trajectories that dwell near the gravitational boundary of two bodies, for instance, are more susceptible to third-body effects. Recent studies also investigate the use of graphical methods<sup>3,4</sup> and extensions of the patched-conic approach to include approximations of three-body motion.<sup>5</sup> However, these approaches are typically intended for specific types of transfers, such as low-thrust and/or gravity assist trajectories. The main drawback of any methodology based on patched-conic approximations is that one cannot guarantee the resulting arcs will lead to reasonable approximations in multi-body regimes during an onboard determination process. Since the startup solution is crucial to

---

\*PhD Candidate, Aerospace Engineering and Engineering Mechanics, The University of Texas at Austin, 210 E. 24th St., Austin, TX 78712. Email: scarritt@mail.utexas.edu

†Assistant Professor, Aerospace Engineering and Engineering Mechanics, The University of Texas at Austin, 210 E. 24th St., Austin, TX 78712. Email: marchand@alumni.purdue.edu

the success of any autonomous iterative targeting process, the present investigation seeks to identify an alternate computational approach for the onboard determination of feasible startup arcs.

The objective of this investigation is twofold: first, to explore the validity of artificial potential function (APF) methods as a possible tool for generating suitable startup solutions; and second, to provide direction for future research by identifying areas of development that can have the most impact on the performance of this method. Artificial potential functions have been used extensively in path planning, for applications ranging from mobile ground robots,<sup>6</sup> to spacecraft formation flight,<sup>7-9</sup> to attitude tracking.<sup>10</sup> They are computationally efficient and simple to implement, making them ideal for onboard use, but they also have inherent limitations in that a continuous control capability is typically assumed and they are also often highly suboptimal. These drawbacks hinder the effectiveness of potential function guidance as a trajectory design tool, since actuation constraints are not uncommon in modern spacecraft missions. Both of these issues can be addressed by autonomous targeters and optimizers. Thus, by using potential function methods to identify the startup arc the user can take advantage of the speed of potential function methods without violating any actuator or mission constraints in the final trajectory.

Artificial potential function guidance is based on the idea that the vehicle environment can be represented mathematically through the definition of potential fields designed to produce some desired vehicle behavior. The general approach is to construct the potential field such that a global minimum exists at the target state while any path constraints, such as obstacles, are assigned higher potentials to discourage the vehicle from traversing those paths. The potential,  $\Phi$ , is written as a nonlinear function of the current position and velocity,  $\mathbf{r}(t)$  and  $\mathbf{v}(t)$ , the desired position and velocity,  $\mathbf{r}_{des}$  and  $\mathbf{v}_{des}$ , and any existing constraints ( $\gamma$ ):

$$\Phi = f(\mathbf{r}(t), \mathbf{v}(t), \mathbf{r}_{des}, \mathbf{v}_{des}, \gamma) \quad (1)$$

Control variables and parameters are subsequently selected such that the vehicle follows the path of steepest descent of the potential. If no local minima exist, convergence to the desired goal state is ensured. In spacecraft applications, potential function methods are used primarily in the field of formation flight. However, the theoretical basis of this method does not preclude the use of potential functions for more general trajectory planning. The key is the construction of the potential. In this study, two-body approximations are utilized as a first step towards constructing a set of artificial potentials that facilitate the identification of trajectories with the desired characteristics. The insight acquired through this analysis is subsequently useful in maneuver planning for the associated startup arc.

## ARTIFICIAL POTENTIAL FUNCTION TRAJECTORY DESIGN

### Potential Function Construction

There are numerous ways to construct the overall potential function for a given problem. Consider, for instance, a transfer between two intersecting orbits. One possible approach would be to accomplish the transfer by executing a maneuver at the point of intersection between the two paths. Subsequently, the following candidate potential is identified,

$$\Phi_{int} = k(\mathbf{r}_{int} - \mathbf{r}_0)^T(\mathbf{r}_{int} - \mathbf{r}_0), \quad (2)$$

where  $\mathbf{r}_0$  is the current position,  $\mathbf{r}_{int}$  is the point of intersection, and  $k$  is a user-defined weight. Designing a potential to achieve a transfer between non-intersecting orbits is more complex. The

approach selected in this study is based on a potential function control algorithm developed for microsattellites.<sup>8</sup> The construction of the artificial potential begins with the creation of a desired velocity field. This is a function of the current state and some desired final target state or path constraint. The potential is then only explicitly a function of the error between the current and desired velocities,

$$\Phi_{vel} = k(\mathbf{v}_t(\mathbf{r}_0, \mathbf{r}_{des}, \mathbf{v}_{des}) - \mathbf{v}_0)^T(\mathbf{v}_t(\mathbf{r}_0, \mathbf{r}_{des}, \mathbf{v}_{des}) - \mathbf{v}_0), \quad (3)$$

where  $\mathbf{v}_0$  is the current velocity at position  $\mathbf{r}_0$ ,  $\mathbf{v}_t$  is the required transfer velocity (at the current position) as computed via the velocity field equations, and  $\mathbf{r}_{des}$  and  $\mathbf{v}_{des}$  are the desired (i.e. target) position and velocity. This simplifies to

$$\Phi_{vel} = k\Delta v^2 \quad (4)$$

which is simply the square of the maneuver cost scaled by some user selected weight  $k$ .

Velocity fields can be constructed to impose any user-defined constraints on the trajectory, both along the path and at the endpoint. The calculation of the appropriate desired velocity, though, can be an extremely complex endeavour. For example, of particular interest in this investigation is the design of a velocity field that guides the trajectory to a specified terminal state. If the transfer time is not specified, targeting a final state is equivalent to targeting a final orbit. Ideally, the computed desired velocity  $\mathbf{v}_t$  at a given initial state minimizes the overall transfer  $\Delta v$ . However, for non-circular orbits, calculation of optimal transfer maneuvers, even between coplanar orbits, is an area of study unto itself.<sup>11-13</sup> Thus, optimization of the desired velocity field is beyond the scope of the present study. Specific details of the velocity field constructions used in this investigation will be discussed with the corresponding examples.

## Maneuver Planning

Typically, path planning via the APF approach is accomplished by defining a virtual force that is equal to the sum of the gradients of each active potential with respect to the current position and velocity of the vehicle.<sup>7</sup> This virtual force yields the desired acceleration vector for the vehicle. This acceleration is then matched as closely as possible by the vehicle's actuators. Naturally, the resulting control history is continuous and unconstrained, a feature that is generally undesirable for the present application. Certainly, the approach is not intended for cases involving discrete control parameters, such as impulsive maneuvers more commonly employed in classical trajectory design. Reconciling APF methods with the use of discrete control has been considered for the problem of spacecraft formation flight,<sup>14</sup> and the present investigation adopts a similar approach. In this case, the time derivative of the potential, rather than the gradient, is selected to identify appropriate locations for impulsive maneuvers. Since the vehicle is constrained to stay on its current orbit until a maneuver is performed, changes in the potential  $\Phi$  can result only from the propagation of the vehicle state. Instead of using actuation to drive  $\Phi$  to some pre-specified value, the algorithm described here seeks the minimum value of  $\Phi$  along the current path. If the current orbit does not intersect the desired orbit, then the potential is based on velocity error and the minimum corresponds to the point at which the desired maneuver will have the lowest  $\Delta v$  cost.

The overall potential field presented here consists of either the intersection potential defined in Equation (2) or the velocity potential in Equation (3). A graphical overview of the full APF maneuver planning algorithm is provided in Figure 1. Following initialization, the algorithm determines

whether or not the vehicle is already on the desired path. If not, the next step is to check whether the vehicle has reached the user-specified maximum allowable number of maneuvers. If additional maneuvers are still permissible, then the current state is propagated forward in time until the necessary conditions for a minimum ( $\frac{d\phi}{dt} = 0$  and  $\frac{d^2\phi}{dt^2} > 0$ ) are met. At that point, a maneuver is performed to match the current velocity to the calculated desired velocity and next iteration of the algorithm begins.

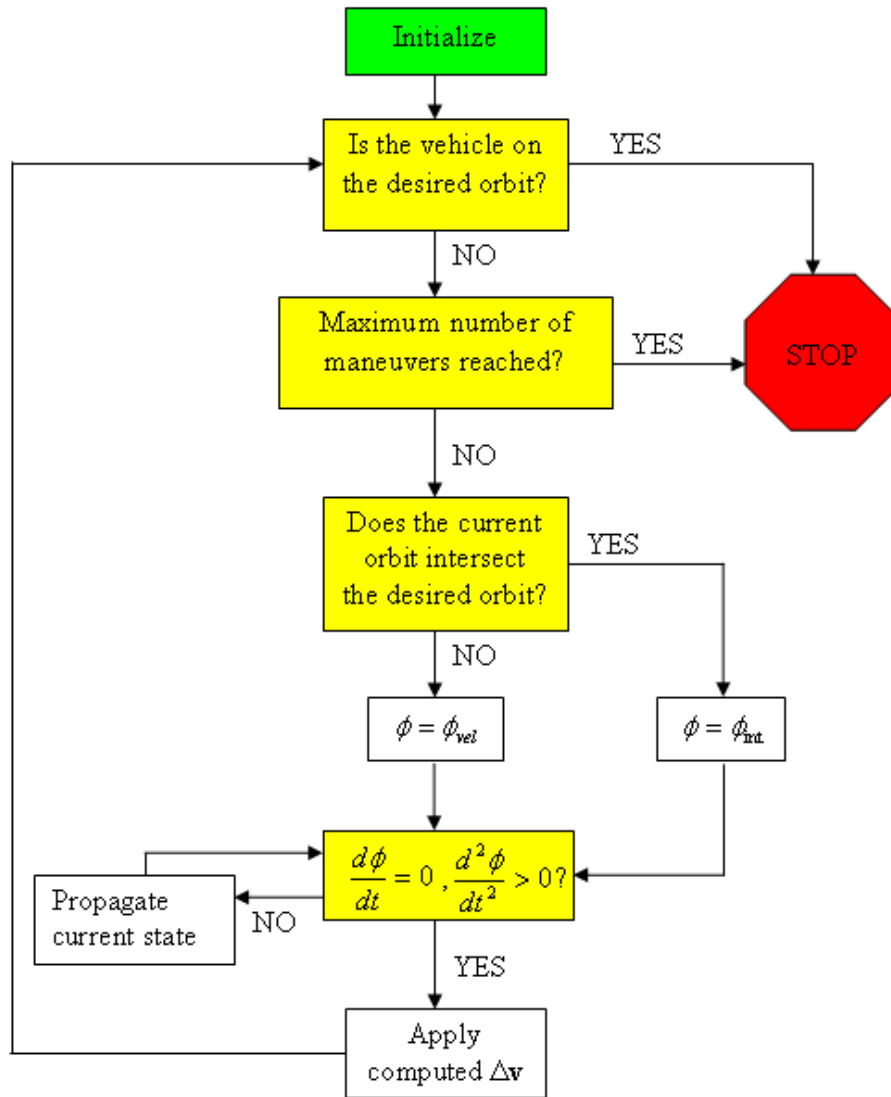


Figure 1. Overview of APF Maneuver Planning

## TRAJECTORY DESIGN EXAMPLES

Initial testing of the APF trajectory design algorithm focuses on transfers in Earth orbit. The first example shown is a simple coplanar transfer, for which the analytical optimal solution is already known. This example provides a useful means for evaluating the performance of APF algorithm

against an established benchmark. Subsequent examples build in complexity; an inclined two-body transfer is examined, followed by a lunar return example that incorporates third-body effects.

To determine the desired velocity field for the following examples, a target point on the final orbit is selected to be an apse of the transfer orbit. If a transfer proceeds from a lower orbit to a higher orbit, then the target point is defined to meet the apoapsis condition. If, instead, the transfer proceeds from a higher orbit to a lower orbit, a periapsis condition is imposed at the target point. Subsequently, the eccentricity vector of the transfer orbit is given by  $\hat{\mathbf{e}}_t$ ,

$$\hat{\mathbf{e}}_t = -\hat{\mathbf{r}}_f, \quad (5)$$

where  $\hat{\mathbf{r}}_f$  is a unit vector aligned with the Earth-to-target line. The magnitude of the target position vector can be determined from the target direction  $\hat{\mathbf{r}}_f$  and the orbital parameters of the desired orbit. The vector  $\hat{\mathbf{e}}_t$  can be used along with the initial and final positions,  $\mathbf{r}_0$  and  $\mathbf{r}_f$ , to compute the eccentricity of the transfer as follows:

$$e_t = \frac{r_f - r_0}{\mathbf{r}_0^T \hat{\mathbf{e}}_t - \mathbf{r}_f^T \hat{\mathbf{e}}_t}. \quad (6)$$

From two-body analysis, the desired velocity  $\mathbf{v}_t$  is then given by

$$\mathbf{v}_t = \frac{1}{r_0^2} \sqrt{\frac{\mu}{r_0 + e_t \hat{\mathbf{e}}_t^T \mathbf{r}_0}} \left[ e_t \left( (\hat{\mathbf{h}}_0 \times \hat{\mathbf{e}}_t)^T \mathbf{r}_0 \right) \mathbf{r}_0 + \left( r_0 + e_t \hat{\mathbf{e}}_t^T \mathbf{r}_0 \right) (\hat{\mathbf{h}}_0 \times \mathbf{r}_0) \right]. \quad (7)$$

### Coplanar Transfer

Selection of the target point depends on the relative geometry of the initial and final orbits and can include numerous factors, particularly for more complex transfers involving third-body perturbations. For the purpose of this investigation, only the orbital planes are considered when designating  $\hat{\mathbf{r}}_f$ . In no plane change is required, the target point is chosen to be the position on the desired orbit that is directly opposite the current position, so that

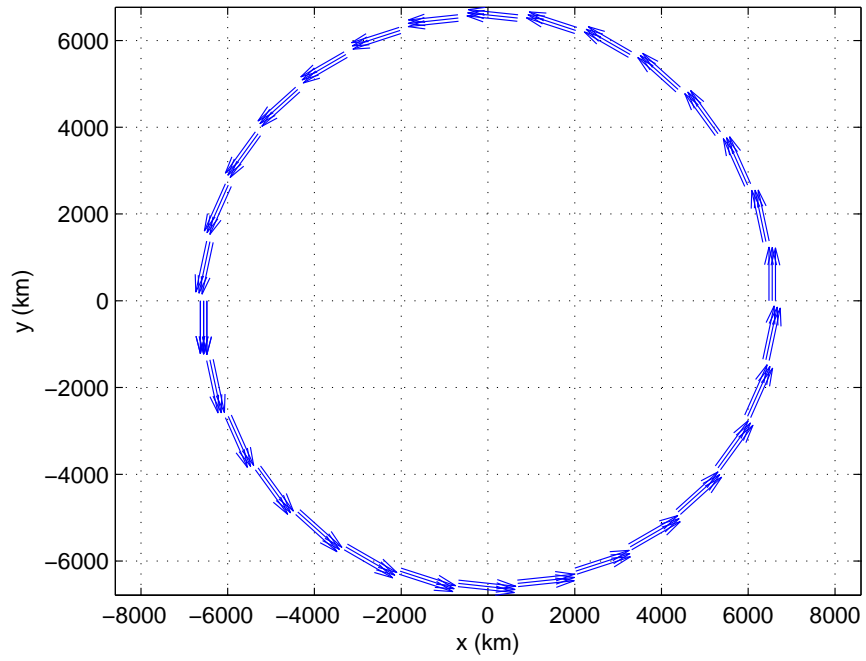
$$\hat{\mathbf{r}}_f = -\frac{\mathbf{r}_0}{r_0}. \quad (8)$$

This choice of  $\hat{\mathbf{r}}_f$  ensures that the transfer angle is always  $180^\circ$ . For the case of two circular orbits, this results in a Hohmann transfer. Figure 2(a) shows the desired velocity field for transfer from a circular equatorial orbit with an altitude of 100 km to an elliptical equatorial orbit with perigee altitude of 400 km. The initial and target states for this transfer are listed in Table 1. The resulting potential, calculated according to Equation (3), is given in Figure 2(b).

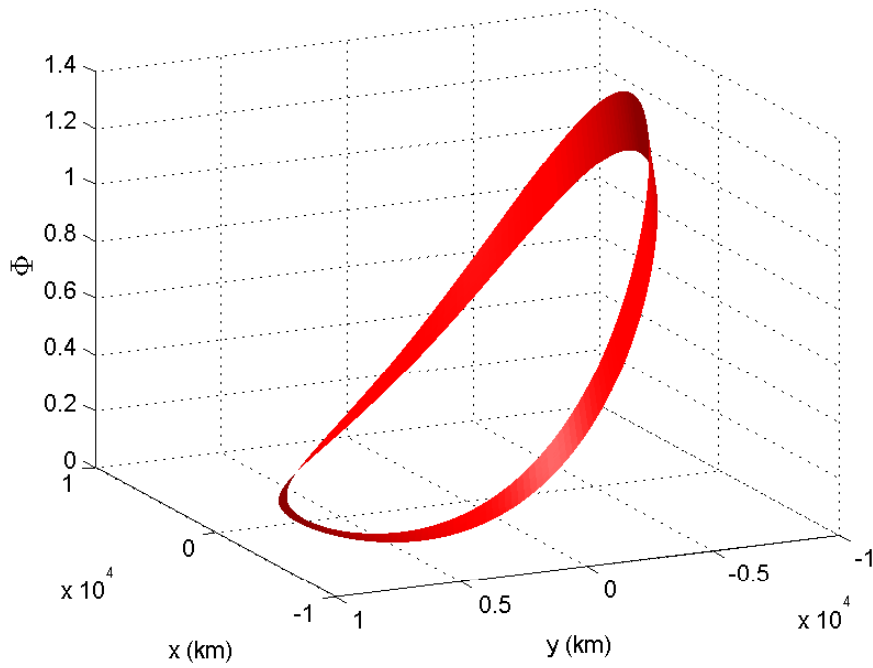
The transfer trajectory that ensues from this potential is shown in Figure 3. An analytical optimal result exists for the coplanar case in the form of a doubly cotangential transfer through an angle of  $180^\circ$ . As Figure 3 shows, the APF method matches this result, which has a total  $\Delta v$  of 1.25 km/s. Although the problem addressed in this example is fairly trivial, the result demonstrates that the APF algorithm is capable of performing on par with analytical methods, when they are available.

### Inclined Transfer

If the initial and desired orbits are not coplanar, the target point is the point where the desired orbit intersects the plane of the initial orbit. This target vector is perpendicular to the angular velocity



(a) Velocity Field



(b) Resulting Potential

**Figure 2. Coplanar Velocity Field and Potential Function**

**Table 1. Coplanar Transfer Initial and Target States**

Parameter	Initial	Target
x (km)	-6478.145	0.000
y (km)	0.000	12587.983
z (km)	0.000	0.0000
$v_x$ (km/s)	0.000	-4.708
$v_y$ (km/s)	-7.844	0.000
$v_z$ (km/s)	0.000	0.000

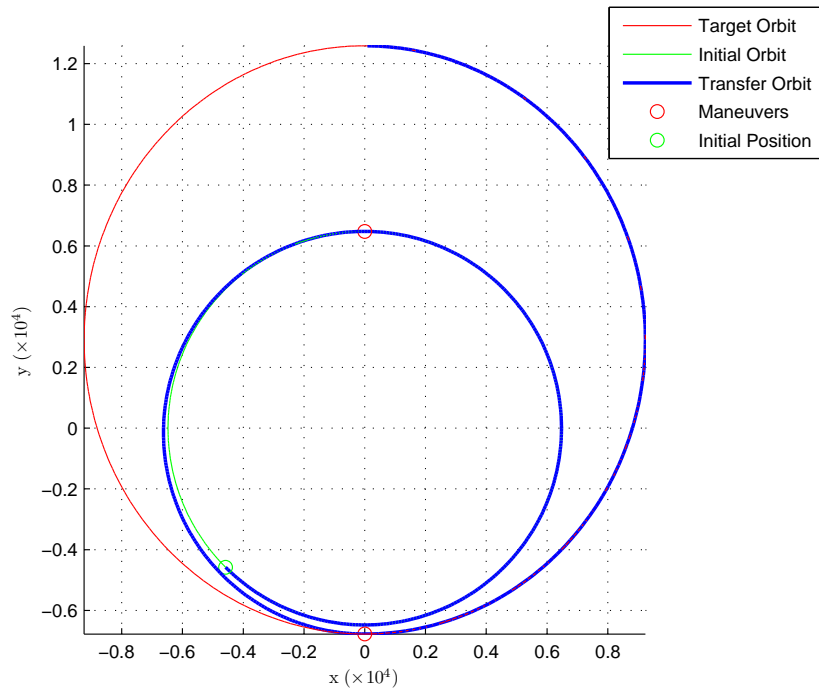


**Figure 3. Coplanar Transfer**

**Table 2. Inclined Transfer Initial and Target States**

Parameter	Initial	Target
x (km)	-5610.238	190.512
y (km)	0.000	12396.744
z (km)	3239.073	2177.562
$v_x$ (km/s)	0.000	-4.690
$v_y$ (km/s)	-7.844	0.000
$v_z$ (km/s)	0.000	0.410

vectors of both orbits, so its direction is given by

$$\hat{\mathbf{r}}_f = \pm \frac{\mathbf{h}_0 \times \mathbf{h}_{des}}{\|\mathbf{h}_0 \times \mathbf{h}_{des}\|}. \quad (9)$$

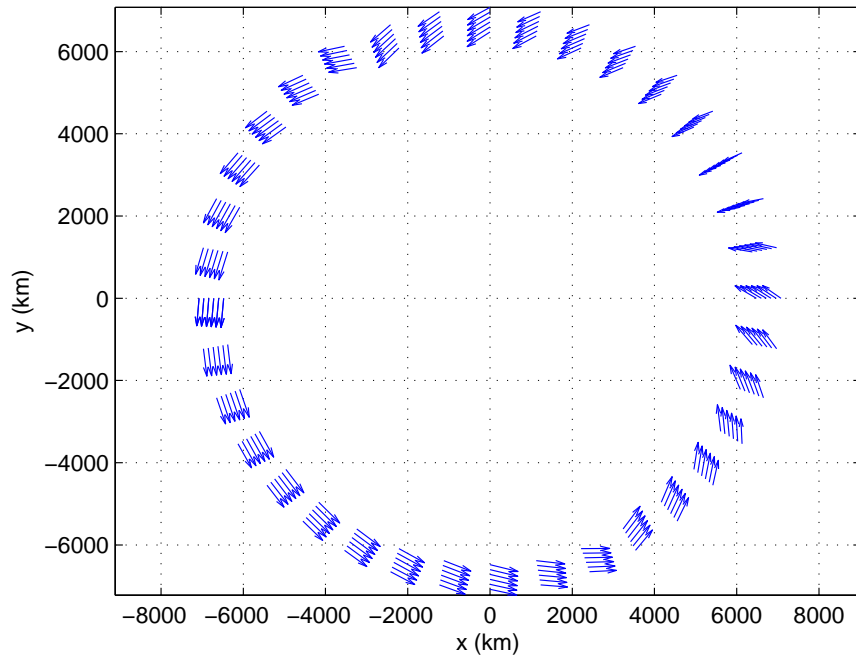
Equation (9) yields two results for the direction of intersection, although both answers may not always be valid depending on the geometry of the two orbits. If two legitimate intersection points do exist, then point with the greater radial distance from the central body is chosen as the target point in order to minimize the  $\Delta v$  resulting from the plane change. An example velocity field and its associated potential are shown in Figures 4(a) and 4(b). The initial and target states for this example are given in Table 2. Note that the potential surface is not smooth as it was in the coplanar case; this is due to a singularity that occurs in the calculation of  $\hat{\mathbf{e}}_t$ , Equation (5), when the initial and final position vectors are exactly aligned. Under these conditions, the resulting transfer orbit is rectilinear.

The non-coplanar transfer, shown in Figure 5, requires a much greater  $\Delta v$  than the coplanar example due to the plane change. This transfer has a total cost of 3.46 km/s, compared to 1.25 km/s for the coplanar example. Using a Lambert targeting algorithm to achieve this same transfer, for the same transfer time, results in a  $\Delta v$  of 6.11 km/s. Because of the high cost incurred by changing the orbital plane, it is often preferable to perform the plane change at a greater radius than the intersection point and then use a third maneuver to put the vehicle on the target orbit.<sup>2</sup> Incorporating this approach to inclined transfers into the APF method should produce significant improvement for cases involving large plane changes; this will be explored further in future studies.

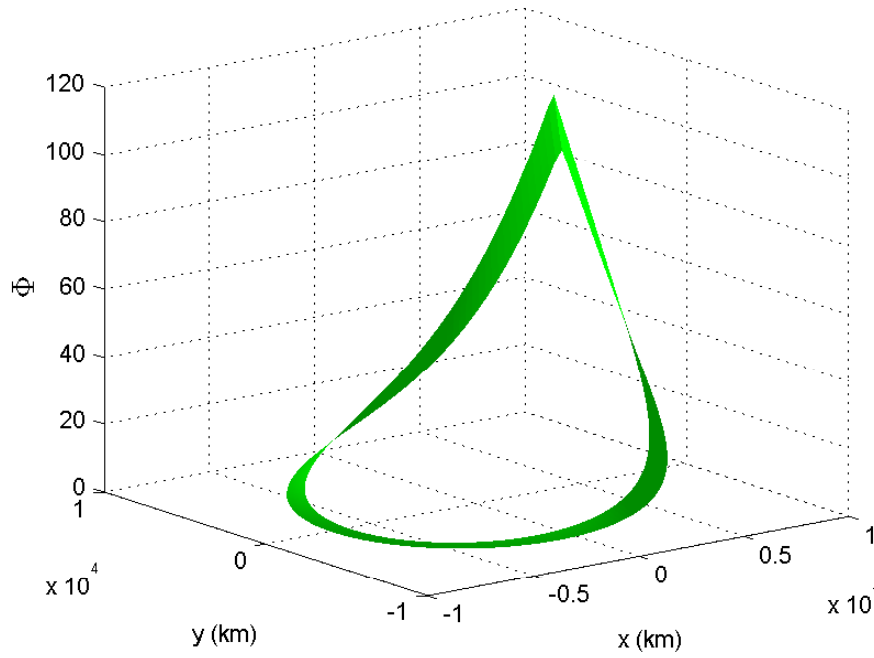
## Lunar Transfer

In order for the APF method to be a useful general tool for identifying startup arcs, it must be able to produce valid results for more complex cases, such as cislunar trajectories. In the examples below, the velocity field construction described previously is employed in the APF algorithm to design a return trajectory from a low-lunar parking orbit. Initial conditions for the parking orbit are listed in Table 3. To determine an appropriate target orbit, i.e. one that will return the spacecraft to some acceptable Earth entry interface, a set of entry constraints is chosen along with an estimated arrival time. These constraints are used to compute the entry state (position and velocity), which is then propagated backwards in time until reaches the lunar sphere of influence. The position and velocity at the end of the propagation are input as the desired final state for the APF algorithm. The entry interface constraints and arrival time for this example are given in Table 4. It should be noted that the timing of the vehicle's arrival at the target state is now significant, as the entry parameters





(a) Velocity Field



(b) Resulting Potential

**Figure 4. Non-Coplanar Velocity Field and Potential Function**

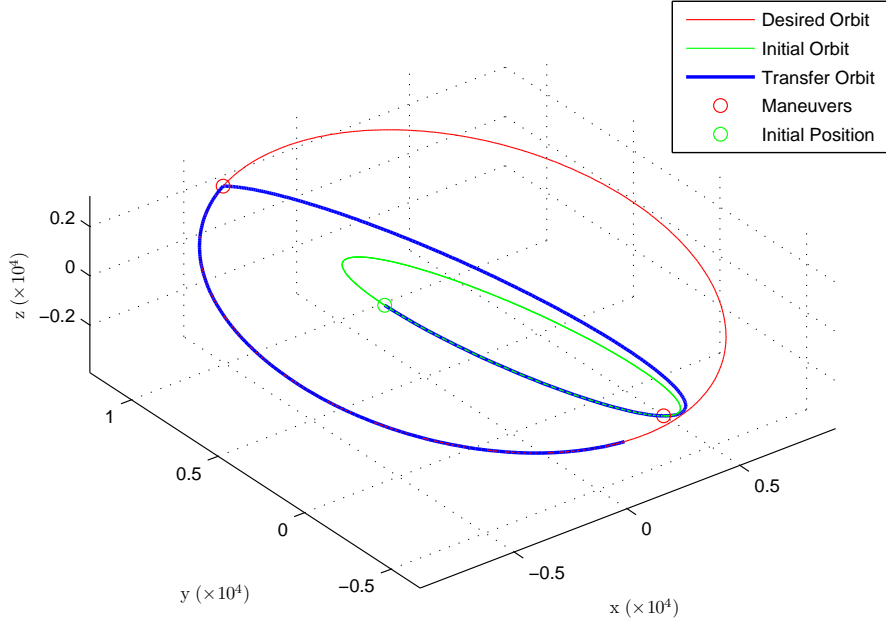


**Figure 5. Non-Coplanar Transfer**

will depend on the relative configuration of the Earth and Moon. Because the current APF method determines maneuvers independent of time, there may exist a mismatch between the assumed time of arrival at the desired state, determined via the backward propagation, and the actual time of arrival of the APF-determined departure trajectory. This is rectified by adjusting the vehicle’s initial departure time through a simple offset targeting algorithm. At each iteration, the arrival time error is computed and that value is subtracted from the current departure time. This method typically reduces the arrival time error to within 1 second in 3 or 4 iterations.

The trajectory generated by the APF algorithm is shown in Figure 6. This arc has a total  $\Delta v$  of 1.9483 km/s, which is high for a lunar return, but this is an issue that can be addressed to some extent by a targeting or optimization algorithm. Ideally, though, the cost of the startup arc should be as low as possible before being passed on to the targeting routine, so it is beneficial to examine ways in which the cost of the APF trajectory can be reduced.

Phasing is extremely important when designing trajectories in multi-body systems. Using two-body approximations to construct the artificial potential field neglects the effects of phasing, a limitation that can have a detrimental effect on the performance of the APF algorithm. Consider the return example described previously. If the departure and entry times for this transfer were shifted, the change in the Earth-Moon configuration could cause a noticeable difference in the trajectory produced by the APF algorithm. To demonstrate this timing effect, the transfer above is subjected to time shifts over a range of  $\pm 12$  revolutions of the initial orbit. These arcs have the same initial conditions and entry parameters as those listed in Tables 3 and 4, except that the epochs for departure and arrival are shifted by  $n$  revolutions. The costs of the resulting transfers are plotted against  $n$  in Figure 7. It is clear from Figure 7 that significant improvements in cost can be achieved for this

**Table 3. Initial Conditions**

Epoch	2-Aug-2018 17:16:06 TDT
x (km)	-1834.7155
y (km)	-66.2361
z (km)	-73.9653
$v_x$ (km/s)	-0.0864
$v_y$ (km/s)	0.8139
$v_z$ (km/s)	1.4136

**Table 4. Estimated Arrival Conditions**

Epoch	7-Aug-2018 00:52:08 TDT
Geocentric Altitude (km)	121.92
Longitude (deg)	-134.5456
Geocentric Latitude	-19.20410
Geocentric Azimuth (deg)	13.9960
Geocentric Flight Path Angle (deg)	-5.8600

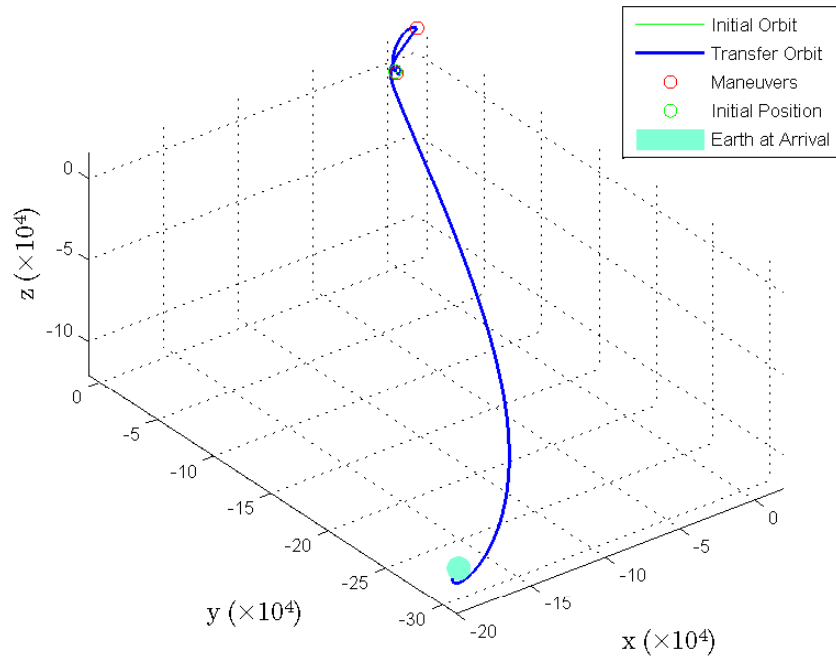


**Figure 6. APF Lunar Return, 1.9483 km/s**

transfer simply by waiting for a few revolutions before departing; the total  $\Delta v$  drops from 1.9843 km/s to 1.5813 km/s, a reduction of over 0.4 km/s, in the course of just 4 revolutions. Conversely, a poor choice of transfer epoch can have a disastrous effect on cost, as evidenced by the 2.6236 km/s trajectory that results from delaying by 2 revolutions. Future iterations of the APF algorithm must be capable of taking these phasing effects into account in order to be truly effective as a general trajectory design tool.

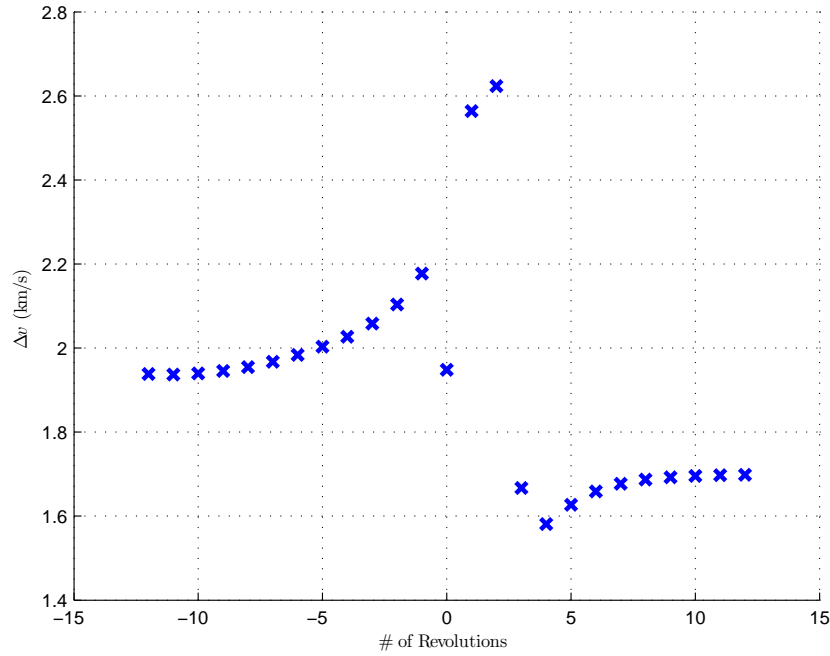


**Figure 7.  $\Delta v$  of Time-shifted Return Trajectories**

## CONCLUSIONS

This investigation examines the use of artificial potential function (APF) methods as a means of identifying suitable startup arcs for targeting and optimization algorithms. The primary objectives of the study are to evaluate the feasibility of this approach for complex trajectory design and to determine key areas of development for future research. Candidate potential functions are defined in terms of a) error between the current position and a desired intersection point on a target orbit and b) error between the current velocity and the desired velocity, and a method for calculating a desired velocity field, based on two-body analysis, is presented. These are employed in the development of a preliminary APF trajectory design algorithm for orbital transfers. This algorithm uses the time derivative of the potential to determine impulsive maneuver locations, rather than the classical APF approach of using the gradient to calculate a desired acceleration vector. The APF design method is utilized to generate sample Earth orbit and lunar return trajectories, and the effect of phasing on the overall trajectory cost is investigated. Results indicate that this method has promise as a tool for fast calculation of startup trajectories, but the current two-body-based potential function construction limits its effectiveness in more complex dynamical systems where timing plays a significant role in the cost and structure of solution arcs. Future work will seek to address this issue through the

development of potentials that incorporate more complex dynamics and can better address issues such as large plane changes and time sensitivity.

## ACKNOWLEDGMENTS

This research was carried out at The University of Texas at Austin and was partially funded under NASA Award Number NNX07AR46G. Any opinions, findings, and conclusions or recommendations expressed in this material are those of the authors and do not necessarily reflect the views of the National Aeronautics and Space Administration.

## REFERENCES

- [1] M. W. Weeks, B. G. Marchand, C. W. Smith, and S. Scarritt, "Onboard Autonomous Targeting for the Trans-Earth Phase of Orion," *Journal of Guidance, Control, and Dynamics*, May-June.
- [2] J. Prussing and B. Conway, *Orbital Mechanics*. New York, NY: Oxford University Press, 1993.
- [3] N. J. Strange and J. M. Longuski, "Graphical Method for Gravity-Assist Trajectory Design," *Journal of Spacecraft and Rockets*, Vol. 39, No. 1, 2002, pp. 9–16.
- [4] A. E. Petropoulos and J. M. Longuski, "Shape-Based Algorithm for Automated Design of Low-Thrust, Gravity-Assist Trajectories," *Journal of Spacecraft and Rockets*, Vol. 41, No. 5, 2004, pp. 787–796.
- [5] R. S. Wilson and K. C. Howell, "Trajectory Design in the Sun-Earth-Moon System Using Lunar Gravity Assists," *Journal of Spacecraft and Rockets*, Vol. 35, No. 2, 1998, pp. 191–198.
- [6] J. Savage, E. Marquez, J. Pettersson, N. Trygg, A. Petersson, and M. Wahde, "Optimization of waypoint-guided potential field navigation using evolutionary algorithms," *IEEE/RSJ International Conference on Intelligent Robots and Systems*, Sendai, Japan, Sept. - Oct. 2004, pp. 3463 – 3468.
- [7] A. Tatsch and N. Fitz-Coy, "Dynamic Artificial Potential Function Guidance for Autonomous On-Orbit Servicing," *6th International ESA Conference on Guidance, Navigation and Control Systems*, Loutraki, Greece, Oct. 2005.
- [8] M. Swartwout, S. Scarritt, and J. Neubauer, "Potential Function Controllers for Proximity Navigation of Underactuated Spacecraft," *Advances in the Astronautical Sciences*, Vol. 128, 2007, pp. 267–286.
- [9] J. Neubauer, *Controlling Swarms of Micro-Utility Spacecraft*. PhD thesis, Washington University in St. Louis, August 2002.
- [10] G. R. Massimo Casasco, "Time-Varying Potential Function Control for Constrained Attitude Tracking," *Advances in the Astronautical Sciences*, Vol. 119, No. 1, 2004, pp. 555–574.
- [11] D. F. Lawden, "Optimal Transfers Between Coplanar Elliptical Orbits," *Journal of Guidance, Control, and Dynamics*, Vol. 15, No. 3, 1992, pp. 788–791.
- [12] R. A. Broucke and A. F. B. A. Prado, "Optimal N-Impulse Transfer Between Coplanar Orbits," *Advances in the Astronautical Sciences*, Vol. 85, 1993, pp. 483–502.

- [13] S. A. Stanton, "Optimal Orbital Transfer Using a Legendre Pseudospectral Method," Master's thesis, Massachusetts Institute of Technology, August 2003.
- [14] C. R. McInnes, "Autonomous Path Planning for On-Orbit Servicing Vehicles," *Journal of the British Interplanetary Society*, Vol. 53, 2000, pp. 26–38.